

## Measurement of the weak mixing phase $\phi_s$ through time-dependent CP-violation in $B_s^0 \rightarrow J/\psi\phi$ decays in the ATLAS detector

Vladimir Nikolaenko  
on behalf of the ATLAS Collaboration

*Institute for High Energy Physics of NRC Kurchatov Institute,  
142281, Protvino, Moscow region, Russian Federation  
Vladimir.Nikolaenko@cern.ch*

Received 28 February 2020  
Accepted 6 November 2020  
Published 18 December 2020

A measurement of  $B_s$  decay parameters using data collected by the ATLAS detector in  $pp$  collisions at 13 TeV in 2015–2017 is performed. Integrated luminosity of this sample is  $80.5 \text{ fb}^{-1}$ . The measurement of physical parameters are statistically combined with results obtained from Run 1 data at 7 and 8 TeV. The measured value of CP-violating phase  $\phi_s = -0.076 \pm 0.034 \text{ (stat.)} \pm 0.019 \text{ (syst.)}$  is obtained, which has significantly better precision in comparison with Run 1 result. Precision of other physical parameters is also improved, including the decay width difference  $\Delta\Gamma$ . Further improvement is expected from the use of full Run 2 statistics, as well as from modifications in the analysis.

*Keywords:*  $B$  physics; CP violation; flavor physics.

PACS number: 14.40.Nd

### 1. Introduction

The data were collected in 2015–2017 (Run 2), in data taking periods with different instantaneous luminosity, therefore several triggers were applied. All of them were based on the identification of a  $J/\psi \rightarrow \mu^+\mu^-$  decay. Selection criteria for dimuons transverse momenta and trigger prescaling factors varied during the physics run, is dependent on the instantaneous luminosity. If there is at least one muon with transverse momentum greater than  $6 \text{ GeV}/c$  and another muon with transverse momentum greater than  $4 \text{ GeV}/c$  and the instantaneous luminosity is low, then this event was accepted by first-level trigger. Tighter requirements on the muon transverse momenta were applied during high instantaneous luminosity, at the beginning of physics data taking after LHC filling. No lifetime selection was applied in the trigger.

It is worth mentioning some modifications in the detector and in quality control. A new IBL detector was installed close to new beam tube, which improves the precision of lifetime measurement. Apart from the dimuon trigger, a supplementary three-muon trigger was tested and implemented during the 2017–2018 data taking periods, which permitted to collect more events with semileptonic decay of second  $B$ -hadron in event and improve the tagging of  $b$ -quark (or antiquark) in the  $B_s$  meson at production time. Regular control of the offline trigger quality was arranged, based on an express analysis of charged  $B^\pm$  candidates.

Like the  $K^0$  mesons,  $B_s$  meson exists in CP-even and CP-odd states with different lifetimes. The  $\Delta\Gamma_s$  is a difference between inverse lifetimes. CP-odd state has a longer lifetime in comparison with the CP-even one, the relative difference is  $\sim 13\text{--}17\%$ . New phenomenon in comparison with  $K^0$  meson is observation of  $(b\bar{s} \leftrightarrow \bar{b}s)$  oscillations via box diagrams with intermediate  $u$ ,  $c$ ,  $t$ ,  $q\bar{q}$  pairs in  $t$ -channel. The mass difference between heavy ( $B^H$ ) and light ( $B^L$ ) CP-eigenstates leads to measured oscillation frequency with  $\Delta m_s \sim 17.77 \text{ ps}^{-1}$ . CP-violating phase  $\phi_s$  manifests itself in interference terms between mixing and decay amplitudes (nondiagonal elements in time-dependent partial wave analysis).

In the Standard Model, CP-violating phase  $\phi_s \approx 2\beta_s$ , where  $\beta_s$  is angle in the Kobayashi–Maskawa triangle,

$$\beta_s = \arg \frac{-V_{ts}V_{tb}^*}{V_{cs}V_{cb}^*}. \quad (1)$$

There are Standard Model predictions for CP-violating phase  $\phi_s$  and difference between inverse lifetimes of different CP-states:

$$\phi_s = -0.0363 + 0.0016 - 0.0015 \text{ radian}, \quad (2)$$

$$\Delta\Gamma = 0.087 \pm 0.021 \text{ ps}^{-1}, \quad (3)$$

(see Refs. 1–3). Measurements of  $\phi_s$  and  $\Delta\Gamma$  test the theoretical predictions.

## 2. Experimental Procedure

The analysis of data at 13 TeV is similar for published analysis of 7 and 8 TeV data (Ref. 4). The number of signal events at 13 TeV is greater by a factor of 4 in comparison with Run 1. Due to high statistics, more detailed study of acceptance, signal shape and background was performed. Opposite-side tagging with muons, electrons and jets was applied. Finally, results at 13 TeV were statistically combined with Run 1 measurements.

The following event selection was applied. The  $J/\psi$  candidates were selected using information from inner detector and muon spectrometer. In order to take into account changes in track reconstruction precision in different intervals of tracks pseudorapidity, different selection requirements on dimuon mass candidates were

Measurement of the weak mixing phase  $\phi_s$  through time-dependent CP-violation

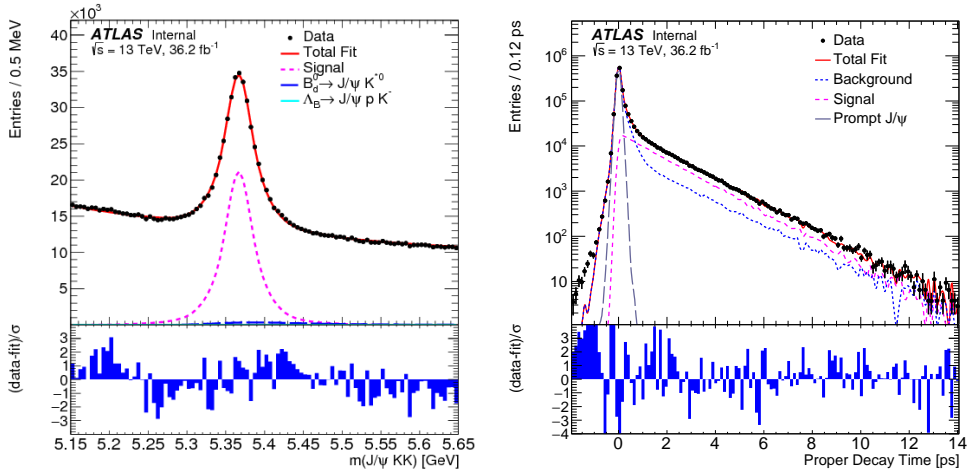


Fig. 1. (Left) Mass distribution of  $B_s \rightarrow J/\psi \phi$  candidates and mass projection of fitted components.  $B_s^0$  signal and background components shown. (Right) Proper decay time fit projection for the  $B_s^0$  sample. Difference between data points and the total fit projections shown on the bottom plots (divided by sum of statistical and systematic errors taken in quadrature).

applied. Pairs of opposite charge tracks with transverse momentum  $p_t > 1.0$  GeV and within pseudorapidity interval  $|\eta| < 2.5$  were taken with kaon mass and considered as  $\phi(1020)$  candidates, when the effective mass of kaon pair  $1008.5 < m(K^+ K^-) < 1030.5$  MeV. Selected four-track combination was used as input for vertex fit, using the  $J/\psi$  mass constraint. Candidates with  $\chi^2/\text{NDF} < 3.0$  were accepted for further analysis. Primary vertex associated with reconstructed  $B_s^0$  candidate was selected with smallest 3D-impact parameter. Then proper decay time of  $B_s^0$  was calculated as

$$t = \frac{L_{xy} M_B}{p_{t_B}}, \quad (4)$$

where  $L_{xy}$  is the  $B_s^0$  impact parameter in transverse plane,  $p_{t_B}$  is the reconstructed transverse momentum of the  $B_s^0$  meson,  $M_B$  is the world-average mass of  $B_s^0$ . There are 3.210 million accepted  $B_s^0$  candidates in mass interval from 5.150 to 5.650 GeV, including  $477240 \pm 760$  events in the fitted  $B_s^0$  signal.

ATLAS uses a right-handed coordinate system with its origin at the nominal interaction point. The  $z$ -axis is along the beam pipe, the  $x$ -axis points to the center of the LHC ring and the  $y$ -axis points upward.

Selected sample of  $B_s^0$  candidates was subjected to time-dependent partial wave analysis, including signal and background models.  $B_s^0$  meson has zero spin, therefore there are three waves in the partial wave analysis of  $B_s^0 \rightarrow J/\psi \phi$  decay (two vectors and angular momentum 0.1 or 2). Apart from decay  $\phi \rightarrow (K^+ K^-)$ , another wave was included with  $K^+ K^-$  system in  $S$ -wave, selected in the same mass interval which was used for  $\phi$  selection.

V. Nikolaenko

The angular basis for partial waves analysis was chosen as follows. The  $\Theta_T$  is the angle between  $\mu^+$  vector and the normal to the  $x - y$  plane, in the  $J/\psi$  meson rest frame. The  $\psi_T$  is the angle between  $K^+$  and inverse vector of  $J/\psi$  momentum in the  $\phi$  meson rest frame. The  $\phi_T$  is the angle between the  $x$ -axis and projection of the  $\mu^+$  momentum to the  $x - y$  plane, in the  $J/\psi$  meson rest frame. The partial wave analysis matrix contains four diagonal and six nondiagonal elements, all of them contain products of angular and time-dependent terms. Detailed description of matrix elements can be found in Ref. 4.

There are two CP-even and two CP-odd waves in the analysis. The CP-violating parameter manifests itself in nondiagonal terms. If there is no information about what was in  $B_s^0$  meson at the production time — was it  $b$ -quark or  $b$ -antiquark, then only terms with  $\cos(\phi_s)$  contribute. If this information is available from the so-called tagging procedure, then other terms appear, which contain  $\sin(\phi_s)$  terms. Since it is known from previous experiments that the absolute value of angle  $\phi_s$  is small, the tagging procedure is very important for getting good precision.

Tagging of  $b$  or  $\bar{b}$  quark in  $B_s^0$  meson is done with information from decay of the second  $B$ -hadron in event. It is the so-called opposite-side tagging, it uses the charge of muon or electron from semileptonic decay of  $b$ -quark. However, there is a background process, with  $b$ -quark decay to  $c$ -quark and then the semileptonic decay of  $c$ -quark which produces a charge muon or electron with opposite sign. The spectrum of leptons from secondary  $c$ -quark decay is soft in comparison with lepton from prompt  $b$ -quark decay. It provides better probability of registration of lepton from  $b$ -decay in comparison with  $c$ -decay.

It was found that the purity of tagging improved if the lepton charge is combined with other charge particles in a cone around the lepton momentum vector. The charges of particles in the cone are averaged, taking the lepton and track charges with weight equal to its transverse momentum. Events with additional track(s) in the cone are considered separately from the case with single leptons. The muon tagging was done separately for tight muons and for low- $p_T$  muons, because the results for two samples are significantly different. The calibration of this method was done of real data, using charged  $B^\pm$  mesons. Possible difference between  $B_s$  and  $B^\pm$  samples was studied in MC events and included to systematic error. The resulting tight muon and electron cone charge distributions and corresponding tagging probability distribution are shown in Figs. 2 and 3. The overlap between events with a muon (either tight or low- $p_T$ ) and events with an electron estimated as 0.6% of tagged events.

If there is neither muon nor electron for the opposite-side tagging, than the jet of charged tracks used for tagging, with jets classified as originating from  $B$ -decay. Tagging power of all methods are presented in Table 1.

The time-dependent partial wave analysis was performed by unbinned likelihood fit with nine physical parameters:  $\phi_s$ , two lifetimes, three independent amplitudes and three so-called “strong phases”  $\delta_\perp$ ,  $\delta_\parallel$ ,  $\delta_\perp - \delta_s$  which arise in decays of  $J/\psi$ ,  $\phi$  and also decay of  $(K^+K^-)$  isobar in  $S$ -wave. A combination of signal

Measurement of the weak mixing phase  $\phi_s$  through time-dependent CP-violation

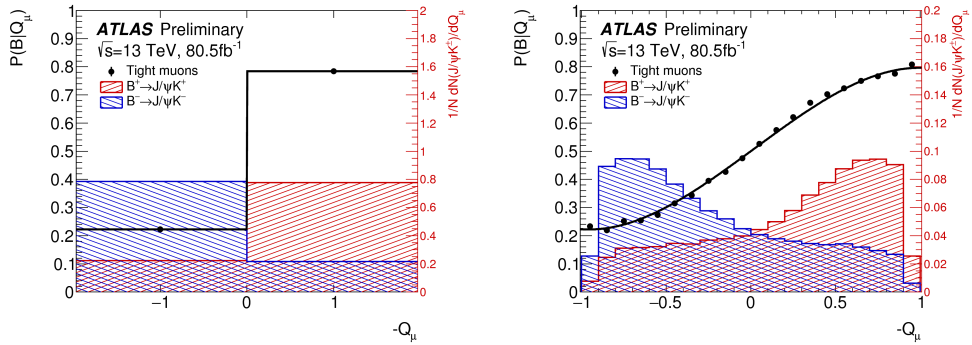


Fig. 2. (Color online) Normalized cone charge distributions for  $B^+$  (in red) and  $B^-$  (in blue) events for tight muons, for cases with single muons (left) and for cases with extra tracks in the cone around muon (right). Tagging probabilities distribution shown by black lines.

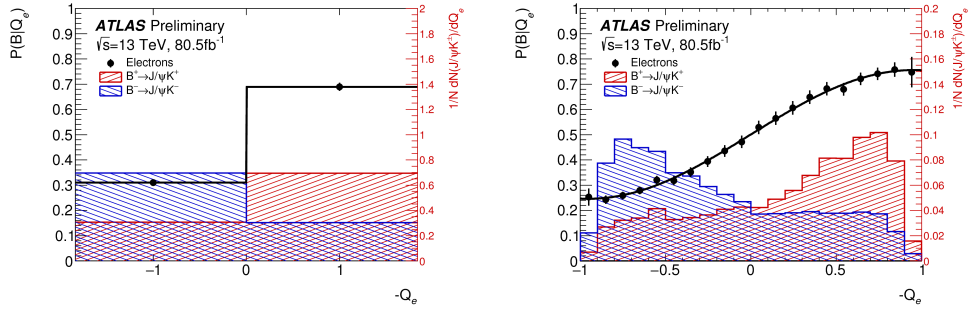


Fig. 3. (Color online) Normalized cone charge distributions for  $B^+$  (in red) and  $B^-$  (in blue) events for electrons, for cases with single electrons (left) and for cases with extra tracks in the cone around electron (right). Tagging probabilities distribution shown by black lines.

Table 1. Summary of tagging power for the different flavor tagging methods on the sample of  $B^\pm$  signal candidates. Uncertainties shown are statistical only.

Tagger	Tagging power [%]
Tight muon	$0.862 \pm 0.009$
Electron	$0.274 \pm 0.004$
Low $p_T$ muon	$0.278 \pm 0.006$
Jet charge	$0.334 \pm 0.006$
Total	$1.75 \pm 0.01$

and background models was constructed. Both models use measured parameters ( $m(J/\psi K^+ K^-)$ , lifetime, decay angles) with errors. It is worth mentioning that there is no lifetime cut in selection of  $B_s$  candidates, the prompt  $J/\psi$  candidates selected together with nonprompt ones. A tail with negative lifetime from prompt  $J/\psi$  is seen in Fig. 1. It permits to keep under control the precision of  $B_s$  lifetime

V. Nikolaenko

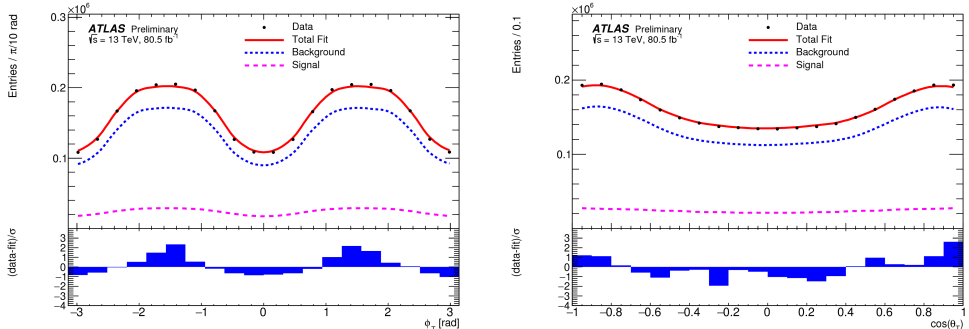


Fig. 4. Angular fit projections (signal, background and sum) for  $\cos(\psi_T)$  and  $\cos(\theta_T)$  angles.

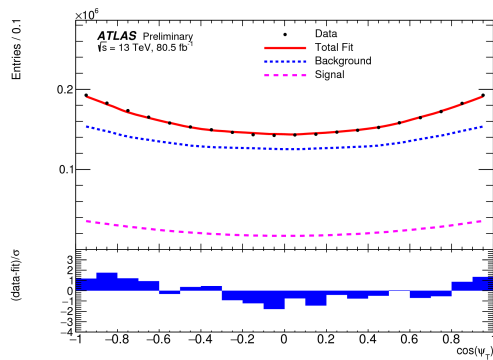


Fig. 5. Angular fit projections (signal, background and sum) for  $\phi_T$  angle.

measurement (a scaling factor was measured and the timing error from reconstruction was multiplied by this factor). The signal model includes a Gaussian function for mass with per-candidate errors, two exponential functions for lifetime (smeared with per-candidate errors) and also tagging probability distributions. The background model apart from the combinatorial background component includes also admixtures from  $B_d$  and  $\Lambda_b$  components. Fractions of misreconstructed components estimated as  $(4.3 \pm 0.5)\%$  from  $B_d \rightarrow J/\psi K^*(980)$  decay and  $(2.1 \pm 0.6)\%$  from  $\Lambda_b \rightarrow bpK^-$  in relation to the number of  $B_s$  candidates. The combinatorial mass distribution was described by exponential function (with per-candidate errors); the lifetime term composed from prompt component ( $\pm t$ ) and two exponentials at  $t > 0$ .

The presence of tagging information permits to improve precision of  $\phi_s$  measurement and permits to measure the “strong phases.” It is worth mentioning that the available information permit to measure other parameter  $\Delta m_{B_s}$ , associated with oscillation frequency of  $B_s$  meson. But it is not done yet in this analysis, the world average from other experiments used,  $\Delta m_{B_s} = 17.757 \pm 0.021 \hbar \text{ ps}^{-1}$ .

Agreement between data and fit results for angular components is shown in Figs. 4 and 5. A careful study of stability of fit result and the systematic errors was done. Summary of systematic errors is presented in Fig. 6.

Measurement of the weak mixing phase  $\phi_s$  through time-dependent CP-violation

	$\phi_s$ [rad]	$\Delta\Gamma_s$ [ps $^{-1}$ ]	$\Gamma_s$ [ps $^{-1}$ ]	$ A_{\parallel}(0) ^2$	$ A_0(0) ^2$	$ A_s(0) ^2$	$\delta_{\perp}$ [rad]	$\delta_{\parallel}$ [rad]	$\delta_{\perp} - \delta_s$ [rad]
Tagging	$1.7 \times 10^{-2}$	$0.4 \times 10^{-3}$	$0.3 \times 10^{-3}$	$0.2 \times 10^{-3}$	$0.2 \times 10^{-3}$	$2.3 \times 10^{-3}$	$1.9 \times 10^{-2}$	$2.2 \times 10^{-2}$	$2.2 \times 10^{-3}$
Acceptance	$0.7 \times 10^{-3}$	$< 10^{-4}$	$< 10^{-4}$	$0.8 \times 10^{-3}$	$0.7 \times 10^{-3}$	$2.4 \times 10^{-3}$	$3.3 \times 10^{-2}$	$1.4 \times 10^{-2}$	$2.6 \times 10^{-3}$
ID alignment	$0.7 \times 10^{-3}$	$0.1 \times 10^{-3}$	$0.5 \times 10^{-3}$	$< 10^{-4}$	$< 10^{-4}$	$< 10^{-4}$	$1.0 \times 10^{-2}$	$7.2 \times 10^{-3}$	$< 10^{-4}$
$S$ -wave phase	$0.2 \times 10^{-3}$	$< 10^{-4}$	$< 10^{-4}$	$0.3 \times 10^{-3}$	$< 10^{-4}$	$0.3 \times 10^{-3}$	$1.1 \times 10^{-2}$	$2.1 \times 10^{-2}$	$8.3 \times 10^{-3}$
Background angles model:									
Choice of fit function	$1.8 \times 10^{-3}$	$0.8 \times 10^{-3}$	$< 10^{-4}$	$1.4 \times 10^{-3}$	$0.7 \times 10^{-3}$	$0.2 \times 10^{-3}$	$8.5 \times 10^{-2}$	$1.9 \times 10^{-1}$	$1.8 \times 10^{-3}$
Choice of $p_T$ bins	$1.3 \times 10^{-3}$	$0.5 \times 10^{-3}$	$< 10^{-4}$	$0.4 \times 10^{-3}$	$0.5 \times 10^{-3}$	$1.2 \times 10^{-3}$	$1.5 \times 10^{-3}$	$7.2 \times 10^{-3}$	$1.0 \times 10^{-3}$
Choice of mass interval	$0.4 \times 10^{-3}$	$0.1 \times 10^{-3}$	$0.1 \times 10^{-3}$	$0.3 \times 10^{-3}$	$0.3 \times 10^{-3}$	$1.3 \times 10^{-3}$	$4.4 \times 10^{-3}$	$7.4 \times 10^{-3}$	$2.3 \times 10^{-3}$
Dedicated backgrounds:									
$B_d^0$	$2.3 \times 10^{-3}$	$1.1 \times 10^{-3}$	$< 10^{-4}$	$0.2 \times 10^{-3}$	$3.1 \times 10^{-3}$	$1.4 \times 10^{-3}$	$1.0 \times 10^{-2}$	$2.3 \times 10^{-2}$	$2.1 \times 10^{-3}$
$\Lambda_b$	$1.6 \times 10^{-3}$	$0.4 \times 10^{-3}$	$0.2 \times 10^{-3}$	$0.5 \times 10^{-3}$	$1.2 \times 10^{-3}$	$1.8 \times 10^{-3}$	$1.4 \times 10^{-2}$	$2.9 \times 10^{-2}$	$0.8 \times 10^{-3}$
Fit model:									
Time res. sig frac	$1.4 \times 10^{-3}$	$1.1 \times 10^{-3}$	$< 10^{-4}$	$0.5 \times 10^{-3}$	$0.6 \times 10^{-3}$	$0.6 \times 10^{-3}$	$1.2 \times 10^{-2}$	$3.0 \times 10^{-2}$	$0.4 \times 10^{-3}$
Time res. $p_T$ bins	$3.3 \times 10^{-3}$	$1.4 \times 10^{-3}$	$0.1 \times 10^{-2}$	$< 10^{-4}$	$< 10^{-4}$	$0.5 \times 10^{-3}$	$6.2 \times 10^{-3}$	$5.2 \times 10^{-3}$	$1.1 \times 10^{-3}$
<b>Total</b>	$1.8 \times 10^{-2}$	$0.2 \times 10^{-2}$	$0.1 \times 10^{-2}$	$0.2 \times 10^{-2}$	$0.4 \times 10^{-2}$	$0.4 \times 10^{-2}$	$9.7 \times 10^{-2}$	$2.0 \times 10^{-1}$	$0.1 \times 10^{-1}$

Fig. 6. Systematic errors associated with physical parameters.

Table 2. Physical parameters from combination of 13 TeV results with Run 1 measurements.

Parameter	Value	Statistical uncertainty	Systematic uncertainty
$\phi_s$ [rad]	$-0.076$	0.034	0.019
$\Delta\Gamma_s$ ps $^{-1}$	0.068	0.004	0.003
$\Gamma_s$ ps $^{-1}$	0.669	0.001	0.001
$ A_{\parallel}(0) ^2$	0.220	0.002	0.002
$ A_0(0) ^2$	0.517	0.001	0.004
$ A_s ^2$	0.043	0.004	0.004
$\delta_{\perp}$ [rad]	3.075	0.096	0.091
$\delta_{\parallel}$ [rad]	3.295	0.079	0.202
$\delta_{\perp} - \delta_s$	-0.216	0.037	0.010

Physical parameters measured on the 2015–2017 data were statistically combined with Run 1 measurement. Combined values of physical parameters are presented in Table 2.

### 3. Results and Discussion

ATLAS can provide precise measurements in  $B$ -decays, which are relevant for searches of effects beyond SM. CP-violating phase  $\phi_s$  and decay width difference  $\Delta\Gamma_r$  measured on the statistics acquired in 2015–2017 (80.5 fb $^{-1}$ ). This result was combined with previous analysis of Run 1 data (19.1 fb $^{-1}$ ). The following result is obtained:

$$\phi_s = -0.076 \pm 0.034 \text{ (stat.)} \pm 0.019 \text{ (syst.) rad ,}$$

$$\Delta\Gamma_s = 0.068 \pm 0.004 \pm 0.003 \text{ ps}^{-1} .$$

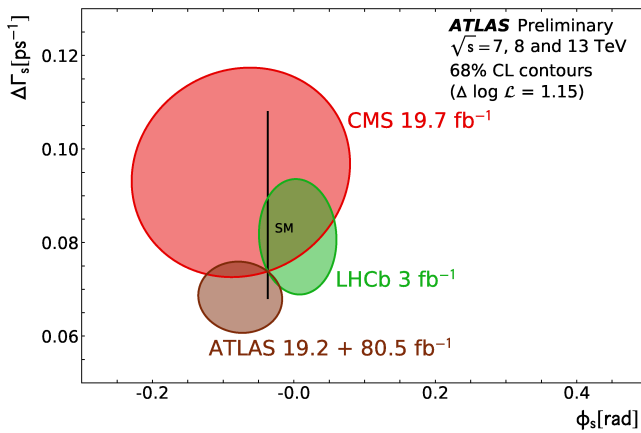


Fig. 7. (Color online) Contours of 68% confidence level in the  $\phi_s - \Delta\Gamma_s$  plane, including results from CMS (red) and LHCb (green) using the  $B_s^0 \rightarrow J/\psi K^+ K^-$  decay only. The blue contour shows the ATLAS result for 13 TeV combined with 7 TeV and 8 TeV. The Standard Model prediction<sup>2,3</sup> is shown as a very thin black rectangle. In all contours the statistical and systematic uncertainties are combined in quadrature.

This measurement can be compared with new LHCb measurement at  $4.9 \text{ fb}^{-1}$  including 2015 and 2016 data in the same decay channel:

$$\begin{aligned}\phi_s &= -0.083 \pm 0.042 \text{ (stat.)} \pm 0.006 \text{ (syst.) rad,} \\ \Delta\Gamma_s &= 0.077 \pm 0.003 \pm 0.003 \text{ ps}^{-1}.\end{aligned}$$

Statistical errors dominate in ATLAS measurements, we expect better precision from analysis of 2018 data due to supplementary statistics and improvements in the analysis.

ATLAS measurement is compared with recent LHCb result (Ref. 6 and with available CMS result, Refs. 7 and 8) in Fig. 7, in the same decay channel. One can see that the ATLAS measurement is consistent with SM prediction and with other experiments.

Results of this study were submitted for publication (Ref. 5). Statistical errors dominate in ATLAS measurements, we expect better precision from analysis of 2018 data due to supplementary statistics and improvements in the analysis.

## References

1. CKMfitter Group (J. Charles *et al.*), *Phys. Rev. D* **91**, 073007 (2015), arXiv:1501.05013, doi:10.1103/PhysRevD.91.073007, (see  $\phi_s$  prediction in Table III).
2. UTfit Collab. (M. Bona *et al.*), *J. High Energy Phys.* **0610**, 081 (2006), doi:10.1088/1126-6708/2006/10/081, (see Table 2,  $\sin(2\beta_s)$ ).
3. A. Lenz and U. Nierste, Numerical updates of lifetimes and mixing parameters of  $B$  mesons, arXiv:1102.4274 [hep-ph].
4. ATLAS Collab. (G. Aad *et al.*), *J. High Energy Phys.* **1608**, 147 (2016), arXiv:1601.03297 [hep-ex], doi:10.1007/JHEP08(2016)147.

5. ATLAS Collab. (G. Aad *et al.*), Measurement of the CP-violating phase  $\phi_s$  in  $B_s^0 \rightarrow J/\psi\phi$  decays in ATLAS at 13 TeV, submitted to *Eurphys. J. C*, arXiv:2001.07115 [hep-ex].
6. LHCb Collab. (R. Aaij *et al.*), *Eur. Phys. J. C* **79**, 706 (2019), arXiv:1906.08356 [hep-ex], doi:10.1140/epjc/s10052-019-7159-8.
7. CMS Collab. (V. Khachatryan *et al.*), Measurement of the CP-violating weak phase  $\phi_s$  and the decay width difference  $\Delta\Gamma_s$  using the  $B_s^0 \rightarrow J/\psi\phi(1020)$  decay channel in  $pp$  collisions at  $\sqrt{s} = 8$  TeV, *Phys. Lett. B* **757**, 97 (2016), arXiv:1507.07527 [hep-ex].
8. CMS Collab., Measurement of the CP-violating weak phase  $\phi_s$  in the  $B_s^0 \rightarrow J/\psi\phi(1020)$ , arXiv:2007.02434 [hep-ex].